

Near infrared photorefractive self focusing in $\text{Sn}_2\text{P}_2\text{S}_6:\text{Te}$ crystals

Cristian Dan,^{1,*} Delphine Wolfersberger,¹ Nicolas Fressengeas,¹ Germano Montemezzani,¹ and Alexander A. Grabar²

¹Laboratoire Matériaux Optiques, Photonique et Systèmes
Unité de Recherche Commune à l'Université "Paul Verlaine" et Supélec - CNRS UMR 7132
2, rue Edouard Belin, 57070 Metz Cedex, France

²Institute of Solid State Physics and Chemistry Uzhgorod National University, Voloshyn
st.54,88000, Uzhgorod, Ukraine

*Corresponding author: Cristian.Dan@metz.supelec.fr

Abstract: The experimental observation of photorefractive self focusing in $\text{Sn}_2\text{P}_2\text{S}_6$: Te crystals at 1.06 μm wavelength is presented. Steady state self focusing is reached as fast as 15 ms for an input peak intensity equal to 160 W/cm^2 . Self focusing is maximum for input peak intensities around 15 W/cm^2 and is decreasing for intensities below and above this value.

© 2007 Optical Society of America

OCIS codes: (190.5330) Photorefractive optics; (190.6135) Spatial solitons; (260.3060) Infrared; (260.5950) Self-focusing

References and links

1. S. Lan, M. F. Shih and M. Segev, "Self-trapping of one-dimensional and two-dimensional optical beams and induced waveguides in photorefractive KNbO_3 ," *Opt. Lett.* **22**(19), 1467 (1997).
2. M. Chauvet, S. Hawkins, G. Salamo, M. Segev, D. Bliss, and G. Bryant, "Self-trapping of planar optical beams by use of the photorefractive effect in InP:Fe ," *Opt. Lett.* **21**(17), 1333 (1996).
3. T. Schwartz, Y. Ganor, T. Carmon, R. Uzdin, S. Shwartz, M. Segev, and U. El-Hanany, "Photorefractive solitons and light-induced resonance control in semiconductor CdZn:Te ," *Opt. Lett.* **27**(14), 1229 (2002).
4. A. A. Grabar, M. Jazbinsek, A. Shumelyuk, Yu. M. Vysochanskii, G. Montemezzani, and P. Günter, chapter *Photorefractive effect in $\text{Sn}_2\text{P}_2\text{S}_6$ in Photorefractive Materials and Their Applications*, vol. 2, J. P. Huignard and P. Günter, eds., pp. 327–362 (Springer, New York, 2007).
5. A. Shumelyuk, S. Odoulov, D. Kip, and E. Krätzig, "Electric-field enhancement of beam coupling in SPS," *Appl. Phys. B* **72**, 707–710 (2001).
6. T. Bach, M. Jazbinsek, P. Günter, A. A. Grabar, I. M. Stoika, and Yu. M. Vysochanskii, "Self Pumped Optical Phase Conjugation at 1.06 μm in Te-doped $\text{Sn}_2\text{P}_2\text{S}_6$," *Opt. Express* **13**, 9890 (2005).
7. A. Shumelyuk, S. Odoulov, O. Oleynik, G. Brost, and A. Grabar, "Spectral sensitivity of nominally undoped photorefractive $\text{Sn}_2\text{P}_2\text{S}_6$," *Appl. Phys. B* **88**, 79–82 (2007).
8. T. Bach, M. Jazbinsek, G. Montemezzani, P. Günter, A. A. Grabar, and Yu. M. Vysochanskii, "Tailoring of infrared photorefractive properties of $\text{Sn}_2\text{P}_2\text{S}_6$ crystals by Te and Sb doping," *J. Opt. Soc. Am. B* **24**, 1535 (2007).
9. A. Zozulya, D. Anderson, A. Mamaev, and M. Saffman, "Solitary attractors and low-order filamentation in anisotropic self-focusing media," *Phys. Rev. A* **57**, 522 (1998).
10. N. Fressengeas, J. Maufoy, and G. Kugel, "Temporal behavior of bidimensional photorefractive bright spatial solitons," *Phys. Rev. E* **54**, 6866–6875 (1996).
11. G. C. Valley, M. Segev, B. Crosignani, A. Yariv, M. M. Fejer, and M. C. Bashaw, "Dark and bright photovoltaic spatial solitons," *Phys. Rev. A* **50**, 4457 (1994).
12. N. Fressengeas, N. Khelifaoui, C. Dan, D. Wolfersberger, G. Montemezzani, H. Leblond, and M. Chauvet, "Roles of resonance and dark irradiance for infrared photorefractive self-focusing and solitons in bi-polar InP:Fe ," Accepted for publication in *Phys. Rev. A*; available for consultation at [arXiv:0705.3521v2](https://arxiv.org/abs/0705.3521v2).

13. A. A. Zozulya and D. Z. Anderson, "Nonstationary self-focusing in photorefractive media," *Opt. Lett.* **20**, 837 (1995).
 14. M. F. Shih, P. Leach, M. Segev, M. H. Garrett, G. J. Salamo, and G. C. Valley, "Two-dimensional steady-state photorefractive screening solitons," *Opt. Lett.* **21**, 324 (1996).
 15. N. Fressengeas, D. Wolfersberger, J. Maufoy, and G. Kugel, "Experimental study of the self-focusing process temporal behavior in photorefractive $\text{Bi}_{12}\text{TiO}_{20}$," *App. Phys.* **85**, 2062 (1999).
-

1. Introduction

Self-trapped beams in photorefractive crystals can generate their own waveguide [1]. Such light guides are especially interesting if they can be generated at near infrared wavelengths and if they can be reconfigured rapidly, which leads to interesting perspectives for applications such as optical routing, steering or switching. At present, much of the interest in near infrared (IR) self focusing and spatial solitons lies on semiconductor materials, because of the small band gap and fast response time [2, 3].

However, the low electro-optic nonlinearity of these crystals (with electro-optic coefficients inferior to 10 pm/V for crystals such as InP, CdTe or GaAs) limit a bit the range of possible applications. Here we present results of near infrared self focusing in a wide band-gap semiconductor with large electro-optic nonlinearity.

The material under investigation is $\text{Sn}_2\text{P}_2\text{S}_6$ (SPS - tin thiohypodiphosphate) with interesting non linear optical properties which makes it suitable for photorefractive (PR) applications: it has a wide optical transparency range (from $0.53\mu\text{m}$ to $8\mu\text{m}$) and a large electro-optic (EO) coefficient that reaches 174 pm/V at room temperature [4]. As a semiconductor type ferroelectric material, SPS combines the large linear electro-optic coefficient characteristic of ferroelectrics and the fast formation of space-charge gratings more typical of semiconductors [4]. Two wave mixing (TWM) experiments have evidenced high gains in near IR: up to 15 cm^{-1} with external applied fields [5] and 4 cm^{-1} without field [6, 7]. The dominating photoconductivity proved to be of the p type [4]. Near infrared optical phase conjugation have shown that SPS response time is more than two order of magnitude faster than that of most conventional photorefractive materials at light intensities of 20 W/cm^2 [6].

Photorefraction in the near IR range ($1.06\mu\text{m}$) has been first demonstrated for nominally pure SPS crystals using pre-exposure with incoherent light [4]. Although a high gain has been obtained, the experiments have shown a strong dependence of the gain on the preexposure time; this disadvantage has been eliminated by doping SPS with tellurium (Te), which, while improving its stability and sensitivity in near IR, also eliminates the electron-hole competition observed in some undoped samples.

While SPS has been widely investigated in wave mixing and phase conjugation configurations up to near infrared wavelengths, to our knowledge no reports about its near IR behavior in a single beam configuration exists. Because of its proven rapid change of refractive index and low absorption at telecom wavelengths, this crystal may become a viable candidate for telecom applications involving reconfigurable optical circuitry such as optical routing.

In this work, we start by investigating the self-focusing behavior at the near IR wavelength of $1.06\mu\text{m}$. We choose Te doped samples with nominal content of 1% because this doping leads to the best IR response in samples that can be grown in a reproducible way [8]. We show that strong self-focusing occurs for moderate applied electric fields and input intensities and investigate its behavior as a function of these parameters. The maximum degree of self-focusing is obtained for an input intensity of 15 W/cm^2 and is less important above and below this level. The steady state is reached as fast as 15 ms for a peak input intensity of 160 W/cm^2 .

2. Experimental setup and crystal parameters

Crystal dimensions are $6 \times 6 \times 11 \text{ mm}^3$ on $X \times Y \times Z$ axis, the convention for the axis presentation being the one described in [4]. *SPS*: Te refractive index at $1.06 \mu\text{m}$ is approximately 2.8 and the X axis is nearly parallel to the direction of the spontaneous polarization axis as presented in [4]. The measured absorption coefficient for the polarization used in the experiments is $\alpha = 0.09 \text{ cm}^{-1}$. No background illumination was used.

A $1.06 \mu\text{m}$ beam polarized along the X axis of the crystal was focused to a waist of $25 \mu\text{m}$ on the crystal entrance face and propagates along the Z direction. Electrodes were deposited on the crystal faces perpendicular to the X axis. For the steady state measurements, the output face was observed using a microscope objective and a CCD camera; for measurements in the transient regime the output face was imaged on a $50 \mu\text{m}$ diameter hole and then recovered and focused with a lens on a photodiode. During the transient regime experiments, the applied field was kept on while the beam was modulated with an acousto-optic modulator (AOM) having a $0.5 \mu\text{s}$ rise time.

The beam power ranged from $10 \mu\text{W}$ to 1.8 mW , thus yielding a peak intensity ranging from approximately 1 W/cm^2 to 180 W/cm^2 . The crystal temperature was maintained at 20°C during the experiments using a Peltier cell. An electric field of 300, 700 and 1000 V/cm respectively was applied in the X direction of the crystal which allows to take advantage of the largest EO coefficient r_{111} of *SPS*.

3. Steady state results

Figure 1 shows a typical result evidencing the self focusing behavior taking place for applied fields ranging from 300 V/cm to 1000 V/cm .

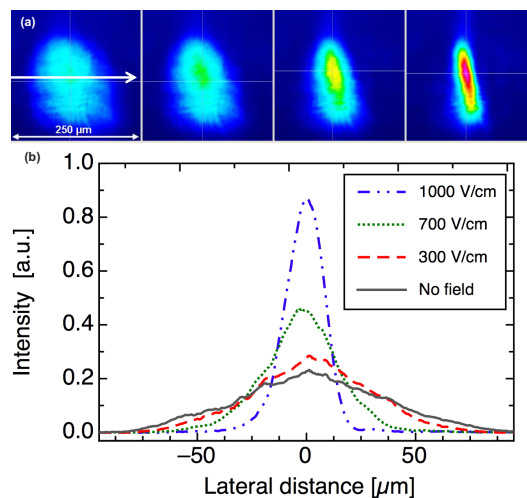


Fig. 1. (a) 2D output beam profile; from left to right: no applied field, 300 V/cm , 700 V/cm and 1000 V/cm ; the arrow indicates the direction of the applied electric field; (b) Output beam profile along the central horizontal line for different applied electric fields. The input power is $200 \mu\text{W}$, corresponding to a 20 W/cm^2 peak intensity. The beam waist is $25 \mu\text{m}$.

As it can be seen in Fig. 1(a), self focusing is strongly dependent on the value of applied electric field and occurs mostly in the direction parallel to the external applied field, while in the vertical direction it is much smaller. Also from beam profiles shown in 1(b) it can be seen

that no significant bending occurs in our sample. Furthermore, if we rotate the light polarization by 90 degrees, we use the lower r_{221} EO coefficient and observe a less important self focusing. For a 1000 V/cm applied field and an input peak intensity of 60 W/cm^2 a horizontal polarized beam focuses to a $19 \mu\text{m}$ radius at the output face of the crystal (the radius is $60 \mu\text{m}$ when there is no applied field), while a vertical polarized beam has a $41 \mu\text{m}$ radius in the same conditions. "Radius" (as used in this work) is the beam half width (in horizontal direction in Fig. 1(a)) at a value of intensity equal to $1/e^2$ from its peak intensity. For our crystal parameters (length and refractive index) the condition for which the input width is equal to the output width is realized for a ratio of 0.4 between output beam radius with and without applied field. Figure 2 shows that this condition is reached (for the direction parallel to the applied field) for an electric field of 1000 V/cm and an intensity of 2 W/cm^2 yet we cannot speak of a 2D spatial soliton because the input beam is circular whereas the output beam is elliptical owing to highly different self focusing ratio for horizontal and vertical directions [9].

The maximum self focusing (minimum beam radius) is obtained for a peak intensity of the order of $10\text{-}20 \text{ W/cm}^2$ (Fig. 2) corresponding to an input power of $100\text{-}200 \mu\text{W}$.

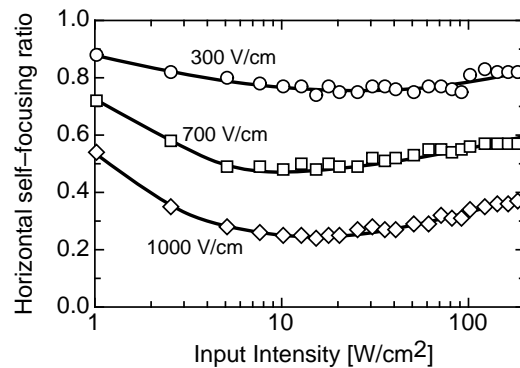


Fig. 2. Steady state self focusing ratio R_1 versus input power for different applied fields measured with the CCD camera. The self focusing ratio is defined as the ratio between output beam radius with and without applied field. The solid curves are guides to the eye.

Below and above this level self focusing is steadily decreasing. This kind of behavior has been already experimentally observed and theoretically modelled in the framework of a single carrier model of photorefractivity [9, 10, 11] and in the case of materials with bipolar conduction [12].

The intensity value for which steady-state self focusing leads to a minimum radius is usually connected to the dark conductivity of the materials through the "dark intensity" I_d . For this intensity the photoconductivity equals the dark conductivity.

We have performed standard current-voltage measurements in our samples to determine the dark conductivity σ_d and the photoconductivity σ_{ph} . At the wavelength and polarization used in our experiments σ_{ph} equals σ_d for an intensity $I = I_d \approx 0.75 \text{ W/cm}^2$. The minimum diameter from Fig. 2 is attained at $I \approx 10\text{-}20 \text{ W/cm}^2$, which corresponds to a ratio $I/I_d \approx 13 - 26$. This value is larger by more than a factor of two with respect to the one predicted by a semi-analytic 2+1 model [9] in the case where a beam is a soliton, which is not satisfied in our case.

4. Transient regime results

In order to characterize the temporal evolution of the self focusing process the output face of the crystal is imaged on a pinhole having a $50 \mu\text{m}$ diameter. At this position, the beam output

radius in the absence of applied field owing to diffraction is $60 \mu\text{m}$, thus part of beam intensity is blocked by the pinhole; when there is an applied electric field the beam is self focused and the output radius is decreased resulting in more light passing through the pinhole. The emerging intensity from the pinhole is measured with a photodiode, which permits to characterize the evolution of the beam radius in real time because there is no significant bending. We have calculated the ratio between intensities passing through the pinhole for different beam sizes under the following assumptions: the self focusing occurs only in the direction parallel to the applied field and the beam maintains its Gaussian profile. We have found that, for the self focusing ratios measured in our case, the intensity recorded by the photodiode is inversely proportional to the beam radius.

For all the measurements, we have chosen to keep the field turned on and to modulate instead the laser beam with a 1Hz repetition rate, meaning that the beam was turned on for half a second and then turned off for another half a second. There was no significant difference between the results given by different pulses; the pulse repetition rate was sufficiently low to permit full relaxation of the refractive index channel. Using an AOM we were able to modulate the beam within less than $0.5\mu\text{s}$ from zero to full power. Figure 3 shows a typical result; the AOM modulation is taken as time origin in our measurements. It can be seen that the recorded radius starts from an initial value (W_i in Fig. 3), decreases with time until reaches a local minimum (W_p) and then increases to a steady state (W_s) which, although larger than the local minimum, is still smaller than the initial value of the radius. This kind of behavior has been theoretically predicted [10, 13] and experimentally observed [14, 15] in other materials.

Using W_p and W_s as defined on Fig. 3 we have performed systematic observations of transient self focusing for different values of incident intensity and applied electric field. Here we are defining the self focusing ratio R_2 at a given time as the ratio between the measured radius at that time when the electric field is on and the value of the radius when there is no applied field.

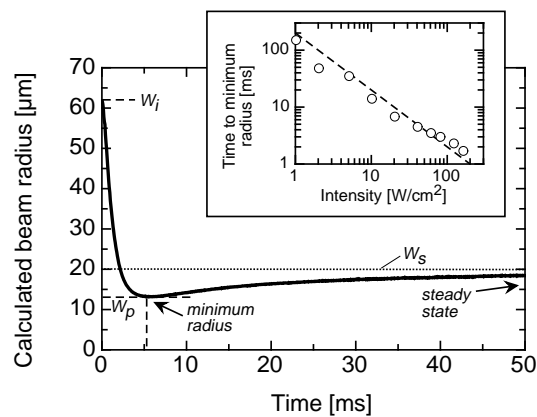


Fig. 3. Self focusing temporal evolution showing transient regime and steady state; W_i is the initial output beam radius (before the beam starts self focusing), W_p is the minimum radius attained during the self focusing and W_s is the radius at steady state. The beam intensity is 40 W/cm^2 , beam input waist is $25 \mu\text{m}$, the applied field is 1000 V/cm . *Inset*: Time needed to reach minimum radius as a function of beam peak intensity. The solid line is a guide to the eye, corresponding to an inverse proportionality.

As it can be seen in Fig. 3 for a 40 W/cm^2 intensity the minimum radius is reached in 5 ms and the steady state in about 50 ms. For 160 W/cm^2 these values are decreased to 2 ms,

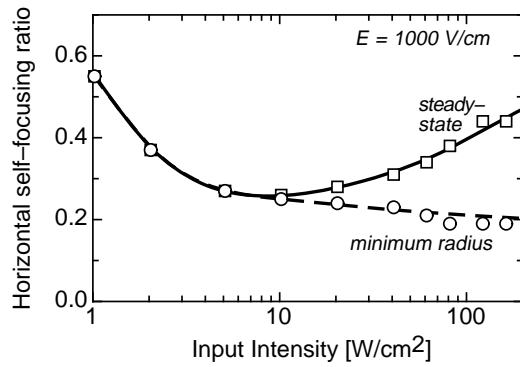


Fig. 4. Self focusing ratio R_2 at minimum radius and at steady state as a function of incident intensity measured with the pinhole-photodiode system. Applied field=1000 V/cm.

respectively 15 ms. The inset in Fig. 3 shows the evolution of the time t_1 needed to reach the minimum radius as a function of peak intensity. The decrease is close to linear, but suggests a slightly sub-linear dependence of t_1 on the inverse intensity. The maximum self focusing (defined as W_p/W_i) and steady state self focusing (W_s/W_i) are shown in Fig. 4 as a function of the incident intensity.

By comparing figures 2 (obtained with the CCD camera) and 4 (obtained with the pinhole-photodiode system) one can see that results obtained with both measurements methods are in agreement: stationary self focusing is maximum for intensities around 15 W/cm². Also from Fig. 4 it can be seen that the transient self focusing maximum is increasing with intensity. Unlike for the steady state, the transient beam radius does not show an increase when the input intensity is increased above 20 W/cm². This transient behavior has been already predicted and observed in other materials [10].

5. Conclusion

Transient and steady-state photorefractive self focusing has been experimentally demonstrated in the near IR for the first time in the highly electro-optic and moderately absorbing $Sn_2P_2S_6$:Te crystal. The output beam diameter has been characterized as a function of applied field and input intensity; its evolution versus intensity has been found to be consistent with available theories. It has been shown that the steady state is reached in less than 15 ms for an input power of 1.6 mW corresponding to a peak intensity of 160 W/cm². The obtained results demonstrate the interest of SPS for the self-focusing of light and the realization of rapidly reconfigurable light-induced wave guides using infrared light for applied voltages much lower than those needed in the case of standard semiconductors.

The authors thank the region Lorraine for their financial support.